




Raman photogalvanic effect: Photocurrent at inelastic light scatteringL. E. Golub  and M. M. Glazov 
Ioffe Institute, 194021 St. Petersburg, Russia (Received 22 July 2022; revised 14 October 2022; accepted 27 October 2022; published 28 November 2022)

We show theoretically that electromagnetic waves propagating in the transparency region of a noncentrosymmetric medium can induce a DC electric current. The origin of the effect is the Raman scattering of light by free carriers in the system. Due to the photon scattering, electrons undergo real quantum transitions resulting in the formation of their anisotropic momentum distribution and in shifts of electronic wave packets giving rise to a steady-state photocurrent. We present the microscopic theory of the Raman photogalvanic effect (RPGE) focusing on two specific situations: (i) generic case of a bulk gyrotropic semiconductor and (ii) a quantum well structure where the light is scattered by intersubband excitations. We uncover the relation of the predicted RPGE and the traditional photogalvanic effect at the light absorption.

DOI: [10.1103/PhysRevB.106.205205](https://doi.org/10.1103/PhysRevB.106.205205)**I. INTRODUCTION**

Photogalvanic effects (PGEs) and photon drag effects (PDEs) resulting in the DC electric current generation under steady-state illumination belong to a class of nonlinear high-frequency transport phenomena, bridge optics, and transport [1–8]. The DC current magnitude and direction depend on the light intensity, propagation direction, and polarization. The processes of the photocurrent generation are highly sensitive to the symmetry of the system, fine structure of the electron energy spectrum, and microscopic processes of the optical transitions and scattering [4,5]. Furthermore, the photocurrent generation can be related in some cases to the topological properties of the charge-carrier Bloch functions [9–13]. It makes polarization-dependent photocurrents an important tool to study the delicate features of the electronic spectrum and kinetic properties of charge carriers in metals and semiconductors and opens up prospects to develop polarization detectors based on these effects [14,15].

Usually, photogalvanic and photon drag currents are observed under the conditions of light absorption, see Fig. 1(a). The PGEs are studied in conventional bulk semiconductors, such as Te and GaAs [4,16], in low-dimensional structures, such as quantum wells [17,18], and in a wide range of emergent material systems including topological insulators [19–24], Weyl semimetals [25,26], graphene-based nanosystems [8,27–29], and transition-metal dichalcogenides [30–32]. Both inter- and intraband optical transitions can be involved in the DC current generation.

It is commonly assumed that, if the light propagates in the transparency region of the crystal, no DC current is formed [4,33,34], although this statement was questioned in recent Refs. [35,36]. It is indeed the case provided real electronic transitions and corresponding changes in the electromagnetic field are absent in the system. In such a situation, the irradiation results solely in renormalization of the energy dispersion. Thus, after a transient process the current van-

ishes [33]; otherwise, in violation of the energy conservation law, such current could generate the Joule heating in the external circuit.

Here we show that even in the absence of photon absorption, the DC electric current can be generated if the light is scattered by the free carriers in the medium. The Raman scattering of light [37,38] leads to the electronic transitions, Fig. 1(b), resulting in the asymmetry of the electron distribution in the steady state and, eventually, in the DC current. A similar idea has been put forward in Ref. [35] without detailed analysis, here we present an explanation of the effect and transparent microscopic model. We develop the microscopic theory of the Raman photogalvanic effect (RPGE) in noncentrosymmetric semiconductors and semiconductor nanostructures. We mainly focus on the case of the circular RPGE where the current reverses its sign under reversal of the radiation helicity. We address the situation where the photon energy is smaller than the fundamental energy gap. We take as examples (i) a nonresonant Raman scattering in bulk semiconductors and (ii) the intersubband resonant Raman scattering in quantum wells. Ultimately, we establish a connection between two fundamental physical processes, the inelastic light scattering, and the electric current generation.

II. GENERAL DESCRIPTION

We recall that the DC current linear in the radiation intensity I arising in the noncentrosymmetric media can be written in the most general form as [4,5]

$$j_{\alpha} = \gamma_{\alpha\beta} i[\mathbf{e} \times \mathbf{e}^*]_{\beta} I + \chi_{\alpha\beta\mu} (e_{\beta} e_{\mu}^* + e_{\mu} e_{\beta}^*) I, \quad (1)$$

where \mathbf{e} is the complex polarization vector of the incident electromagnetic field, $i[\mathbf{e} \times \mathbf{e}^*] = P_{\text{circ}} \hat{\mathbf{n}}$ with P_{circ} being the circular polarization degree and $\hat{\mathbf{n}}$ being the unit vector along the light propagation axis describes the light helicity. Tensors $\gamma_{\alpha\beta}$ and $\chi_{\alpha\beta\mu} = \chi_{\alpha\mu\beta}$ describe circular and linear photocurrents, respectively, α, β, μ are the Cartesian components.

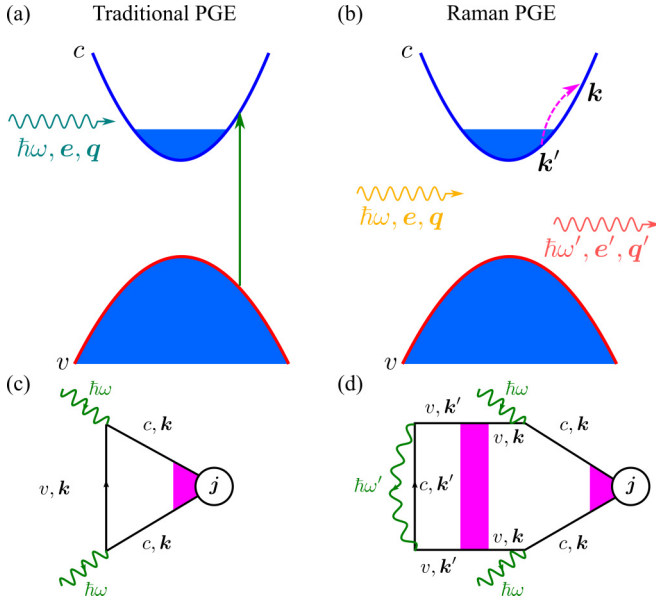


FIG. 1. (a) Scheme of the absorption process leading to circular PGE. (b) Illustration of the scattering process resulting in real electronic transition. (c) and (d) Basic diagrams describing the effects depicted in panels above (see Appendix A for details). The green wavy lines denote the electromagnetic field, \textcircled{j} denotes the current vertex with magenta filling describing the sum of the ladder diagrams accounting for the electron scattering by impurities and phonons. The magenta rectangle denotes the sum of the ladder diagrams accounting for the valence-band hole scattering.

Notably, the first and second terms in Eq. (1) have different properties under time-reversal $t \rightarrow -t$. Particularly, since both current and light helicity change their signs at the time reversal, tensor $\gamma_{\alpha\beta}$ is even and tensor $\chi_{\alpha\beta\mu}$ is odd at $t \rightarrow -t$.

We assume that the light propagates in the transparency region of the direct-gap semiconductor,

$$\hbar\omega < E_g, \quad \omega\tau_p \gg 1, \quad (2)$$

where ω is the frequency of radiation, E_g is the band gap, and τ_p is the conduction electron momentum scattering time. Here, for definiteness, we assume that the system is n doped. The first condition in Eq. (2) ensures that the real interband transitions are forbidden, whereas the second one allows us to neglect the intraband Drude-like absorption. In generic semiconductor systems with $E_g \gtrsim 1$ eV and $\hbar/\tau_p \lesssim 1$ meV both conditions (2) can be readily fulfilled for a wide range of frequency covering almost three orders of magnitude.

Under condition (2) absorption of light is absent, and the only possible real processes are the free-carrier light scattering as illustrated in Fig. 1(a). The incident photon with the frequency $\hbar\omega$, polarization \mathbf{e} , and wave-vector \mathbf{q} scatters and gives rise to a secondary photon with the frequency $\hbar\omega'$, polarization \mathbf{e}' and wave-vector \mathbf{q}' whereas a resident electron undergoes a transition from the \mathbf{k}' to the \mathbf{k} state. Thus, the DC current density can be readily expressed as

$$\mathbf{j} = \frac{e}{\mathcal{V}_0} \text{Tr}\{\hat{v}\rho^{(2)}\} = \mathbf{j}_b + \mathbf{j}_s, \quad (3)$$

with the ballistic,

$$\mathbf{j}_b = \frac{2e}{\mathcal{V}_0} \sum_{\mathbf{k}, \mathbf{k}', \mathbf{q}} [\mathbf{v}_{\mathbf{k}}\tau_p(E_{c,\mathbf{k}}) - \mathbf{v}_{\mathbf{k}'}\tau_p(E_{c,\mathbf{k}'})] \times W_{\mathbf{k}, \mathbf{k}'}^{sc}(\mathbf{e})f_0(E_{c,\mathbf{k}'})[1 - f_0(E_{c,\mathbf{k}})], \quad (4a)$$

and shift,

$$\mathbf{j}_s = \frac{2e}{\mathcal{V}_0} \sum_{\mathbf{k}, \mathbf{k}', \mathbf{q}} \mathbf{R}_{\mathbf{k}, \mathbf{k}'} W_{\mathbf{k}, \mathbf{k}'}^{sc}(\mathbf{e})f_0(E_{c,\mathbf{k}'})[1 - f_0(E_{c,\mathbf{k}})], \quad (4b)$$

contributions, respectively [4,5,39,40]. Here e is the electron charge, \mathcal{V}_0 is the normalization volume, \hat{v} is the velocity operator, and $\rho^{(2)}$ is the electron density matrix calculated in the second order in the incident electromagnetic field amplitude. In Eqs. (4), factors 2 account for the spin degeneracy, $E_{c,\mathbf{k}}$ is the electron dispersion, $f_0(E)$ is the equilibrium Fermi-Dirac distribution function, $\mathbf{v}_{\mathbf{k}} = \hbar^{-1}\partial E_{c,\mathbf{k}}/\partial\mathbf{k}$ is the electron velocity, $W_{\mathbf{k}, \mathbf{k}'}^{sc}(\mathbf{e})$ is the probability of electron scattering $\mathbf{k}' \rightarrow \mathbf{k}$ at the incident light polarization \mathbf{e} averaged over the polarization and propagation direction of the final photon, and $\mathbf{R}_{\mathbf{k}, \mathbf{k}'}$ is the electron shift at the transition $\mathbf{k}' \rightarrow \mathbf{k}$ [41].

The lack of the inversion center allows for odd in the electron wave-vector terms in $W_{\mathbf{k}, \mathbf{k}'}^{sc}(\mathbf{e})$ and even in the wave-vector terms in the $\mathbf{R}_{\mathbf{k}, \mathbf{k}'}$. It makes contributions (4) nonzero. The contribution (4a) has a clear physical interpretation: In the course of quantum transitions electrons acquire an ‘‘average’’ velocity $\bar{\mathbf{v}}$ depending on the light polarization. The velocity generation rate is given by the rate of electron transitions \dot{N} , and the velocity relaxation rate is given by the momentum relaxation rate τ_p^{-1} . As a result, the DC current according to this mechanism is formed during the ballistic propagation of electrons between the scattering events and given by the balance of the generation and relaxation processes [4],

$$\mathbf{j} = e\bar{\mathbf{v}}\tau_p\dot{N}. \quad (5)$$

The shift photocurrent in Eq. (4b) can be estimated in the same manner with the replacement in Eq. (5) $\bar{\mathbf{v}}\tau_p$ by the average shift of the wave-packet $\bar{\mathbf{R}}$ in the course of scattering [4]. Equation (5) underlies that the current generation requires real electronic transitions, and \dot{N} can be expressed via the light intensity and the extinction coefficient \mathcal{K} related to the scattering process $\dot{N} = \mathcal{K}I/\hbar\omega$.

III. MICROSCOPIC MODEL OF THE IMPURITY OR PHONON-ASSISTED RPGE

Now we turn to the microscopic description of the scattering processes. We focus on the photocurrent generation process in the bulk gyrotropic semiconductor under assumption that the incident photon energy is smaller but close to the fundamental band-gap $\Delta = E_g - \hbar\omega \ll \hbar\omega$. In this situation the main contribution to the free-carrier scattering of light is provided by virtual states in the valence band [5]. Accordingly, the scattering can be described as a three-stage process where as shown in Fig. 2(a): (i) the incident photon is absorbed (virtually) and creates an electron-hole pair by promoting the electron with the wave-vector \mathbf{k} from the valence band to the conduction band; (ii) the hole in the valence band scatters (by phonon or impurity) in such a way that the

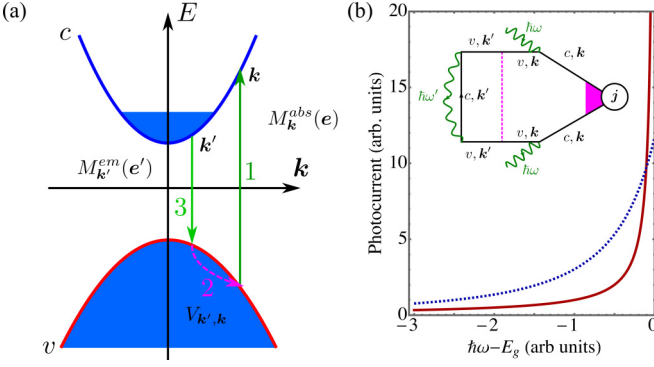


FIG. 2. (a) Scheme of the light scattering process with allowance for the momentum relaxation. (b) Spectral dependence of the photocurrent for a bulk semiconductor (solid line) and quantum wells (dotted line). The inset shows the relevant diagram, see Appendix A.

state k in the valence band becomes filled with electron and the state with the wave-vector k' becomes unoccupied; and (iii) the hole recombines with the resident electron so that finally the valence band remains unperturbed (all the states are filled), and in the conduction band the state with wave-vector k' is empty and the state with wave-vector k is filled. The corresponding scattering rate is given by

$$W_{k,k'}^{sc}(e', e) = \frac{2\pi}{\hbar} \delta(\hbar\omega - \hbar\omega' - E_{c,k} + E_{c,k'}) I \times \left| \frac{M_{k',k}^{em}(e') V_{k,k'} M_k^{abs}(e)}{(\hbar\omega - E_{c,k} + E_{v,k})(\hbar\omega - E_{c,k} + E_{v,k'})} \right|^2, \quad (6)$$

where $M_k^{abs}(e)\sqrt{I}$ and $M_{k'}^{em}(e')$ are the interband transition-matrix elements describing the absorption and emission of photons, respectively, $V_{k,k'}$ is the scattering matrix element in the valence band. It is convenient to present

$$|M_k^{abs}(e)|^2 = |M_0|^2 (1 + D_{\alpha\beta} k_{\alpha} i [e \times e^*]_{\beta}), \quad (7)$$

where the real second-rank tensor $D_{\alpha\beta}$ is responsible for the gyrotropy of the system [4] and M_0 is a constant. The presence of k -linear terms in Eq. (7) makes an odd in the wave-vector contribution to the electron transition rate $W_{k,k'}^{sc}(e) = \sum_{q', e'} W_{k,k'}^{sc}(e', e)$ and eventually results in the nonzero photocurrent Eq. (4b). Equations (4a) and (6) correspond to the diagram in Fig. 2(b). Assuming that the carrier's momentum relaxation is caused by short-range impurities, introducing ξ as the ratio of the conduction- and valence-band elastic-scattering matrix elements squared, and γ_r as the radiative decay rate of the photoexcited electron-hole pair, we obtain the following expression for the circular photocurrent (see Appendix B for technical details of the derivation),

$$j_{\alpha} = en_e \gamma_r D_{\alpha\beta} \hat{n}_{\beta} P_{\text{circ}} I \left| \frac{M_0}{\Delta} \right|^2 \frac{\xi \Phi(\nu)}{3\pi}. \quad (8)$$

Here n_e is the electron density in the conduction band, $\nu = 1 + m_e/m_h$ with m_e and m_h being the electron and hole effective masses, and

$$\Phi(\nu) = \frac{(\nu + 1) \ln \nu - 2(\nu - 1)}{(\nu - 1)^3}.$$

In derivation of Eq. (8) we assumed degenerate electrons with their Fermi energy $E_F \ll \Delta$; the general expression is more bulky but demonstrates similar spectral behavior. The photocurrent in Eq. (8) increases with decreasing the detuning Δ because the smaller Δ is, the more efficient the light scattering is, see Fig. 2(b).

The ballistic photocurrent (8) changes its sign at reversal of the radiation helicity, and Eq. (8) describes the circular RPGE. To obtain the ballistic linear RPGE one has to go beyond the three-stage process described above and take into account additional scattering processes to ensure the correct properties of the current under time reversal or evaluate the shift contribution, Eq. (4b), see Ref. [41] for evaluation of $R_{k,k'}$ for multiquantum transitions. In any case, the linear RPGE will have an additional smallness $\sim (\Delta\tau_p/\hbar)^{-1}$, $(\omega\tau_p)^{-1}$, and $(E_F\tau_p/\hbar)^{-1}$ depending on the particular mechanism of the effect.

It is worth mentioning that the main contribution to the Raman scattering of light by free charge carriers in semiconductors does not require an additional transition of the hole in the valence band. The electron wave vector can change due to the variation of the light wave vector in the course of scattering,

$$k - k' = q - q'. \quad (9)$$

This process is described by the diagram analogous to that in Fig. 2(b) but without the dashed vertical line. The momentum transfer in the course of scattering results in additional contributions to the photocurrent akin to the photon drag effect in the absorption region. An estimate for the such drag contribution can be obtained from Eq. (5) with [see Appendix C, Eq. (C3)]

$$\bar{v} \sim \frac{\hbar q}{m_e}. \quad (10)$$

This contribution is polarization independent.

The circular-polarization-dependent photocurrent arises in the next order in the photon wave vector. Calculation in Appendix C shows that the resulting circular photocurrent differs from that derived above in Eq. (8) by a factor of $\hbar q^2 \tau_p / m_e \ll 1$. The smallness of such a contribution is related to the fact that, in the absence of additional scattering of the hole, the initial and final wave vectors of electrons are close to each other, see Eq. (9): The electron wave vector cannot change more than by a radiation wave vector. It results in a significant reduction of the effect.

IV. RPGE AT THE INTERSUBBAND RESONANCE IN QUANTUM WELL STRUCTURES

Additional specifics of Raman scattering of light appears where the change of the photon frequency corresponds to a frequency of a resonant excitation in the system. Such a situation can naturally arise in quantum well structures as shown in Fig. 3 under conditions of the intersubband scattering [5]. We consider for simplicity a symmetric structure with lowest occupied conduction subband ($c1$). As before the frequency of incident photon corresponds to the transparency region of the structure, Eq. (2) and E_g in this case corresponds to the gap between the topmost \hbar -subband $v1$ and the bottom

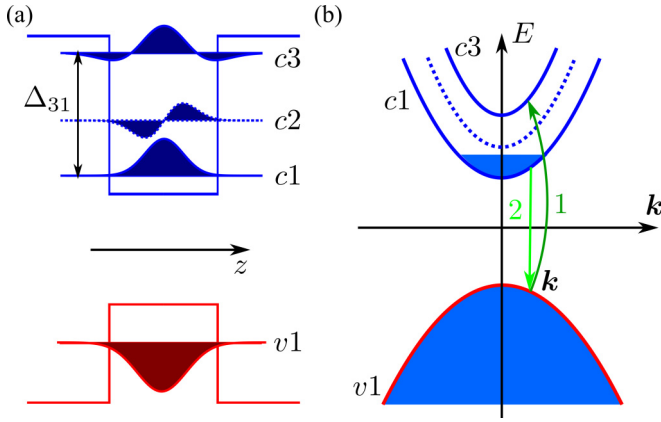


FIG. 3. (a) Quantum well structure. (b) Scheme of the intersubband resonant light scattering process.

conduction-subband $c1$. A situation of interest occurs in the vicinity of the intersubband resonance,

$$\hbar\omega - \hbar\omega' = E_{c3,k} - E_{c1,k}, \quad (11)$$

where the process depicted in Fig. 3(b) becomes possible. In this case the virtual photon absorption via $v1 \rightarrow c3$ electron transition is followed by the photon emission process resulting from the $c1 \rightarrow v1$ transition. As a result, an electron is promoted from the $c1 \rightarrow c3$ subbands (in asymmetric quantum wells similar transitions involving the $c2$ subband are also allowed). The corresponding transition rate is readily evaluated [cf. Eq. (6)]

$$W_{3 \leftarrow 1}^{sc}(\mathbf{e}', \mathbf{e}, \mathbf{k}) = \frac{2\pi}{\hbar} \left| \frac{M_{\mathbf{k}}^{em}(\mathbf{e}') M_{\mathbf{k}}^{abs}(\mathbf{e})}{\hbar\omega - E_{c3,k} + E_{v1,k}} \right|^2 \times \delta(\hbar\omega - \hbar\omega' - E_{c3,k} + E_{c1,k}) I. \quad (12)$$

We neglect the photon momentum and any additional phonon or impurity scattering processes, hence, the transitions take place at the same electron wave-vector \mathbf{k} . As above we focus on the ballistic circular RPGE because it dominates the photocurrent and using the same Eq. (7) for $|M_{\mathbf{k}}^{abs}(\mathbf{e})|^2$ as in the bulk case we arrive at the following expression for the current density (see Appendix D for details):

$$j_{\alpha} = -en_e \gamma_r^{QW} D_{\alpha\beta} \hat{n}_{\beta} P_{circ} I \frac{|M_0|^2 \tau_{tr}}{\nu_{31} \Delta_{QW} \hbar} \chi(\varepsilon). \quad (13)$$

Here γ_r^{QW} is the recombination rate of the electron in the $c1$ subband with the $v1$ hole, we assumed the parabolic dispersion $E_{c1,k} = \hbar^2 k^2 / 2m_{c1}$, $E_{c3,k} = \Delta_{31} + \hbar^2 k^2 / 2m_{c3}$ with m_{ci} ($i = 1, 3$) being the effective mass in the i th subband, and Δ_{31} being the intersubband energy gap. In Eq. (13) we have introduced $\nu_{31} = m_{c1}/m_{c3} + m_{c1}/m_h$, τ_{tr} is the momentum scattering time of the $c1$ electron at a Fermi surface, the detuning for quantum wells $\Delta_{QW} = E_g + \Delta_{31} - \hbar\omega$, and

$$\varepsilon = \frac{\Delta_{QW}}{\nu_{31} E_F}, \quad \chi(\varepsilon) = \varepsilon \left(\ln \frac{1 + \varepsilon}{\varepsilon} - \frac{1}{1 + \varepsilon} \right). \quad (14)$$

Equation (13) is valid for degenerate electrons and under assumption that the momentum relaxation in the $c3$ subband is much faster than in the $c1$ subband: It is typically the

case because of optical phonon emission processes causing electrons to relax to the bottom subbands; the general case is considered in Appendix D. It follows from Eq. (13) that the RPGE current at the intersubband scattering tends to a constant at the absorption edge being much weaker function of the detuning as compared to the analogous photocurrent in the bulk, cf. Eq. (8) and Fig. 2.

V. DISCUSSION

A. Comparison with circular PGE in the absorption region

It is instructive to compare the results for the circular photocurrent obtained here for the transparency region with the well-known results for the circular PGE at the direct interband transitions. Considering the bulk semiconductor in the model described above [see the diagram in Fig. 1(c)] we obtain the following expression for the conduction electron photocurrent at $\hbar\omega > E_g$:

$$j_{\alpha}^{abs} = e \frac{\mathcal{A} I}{\hbar\omega} D_{\alpha\beta} \hat{n}_{\beta} P_{circ} \frac{2|\Delta| \tau_p}{3\nu^2 \hbar}. \quad (15)$$

Here \mathcal{A} is the absorption coefficient of the semiconductor, the electron momentum scattering time τ_p is taken at the energy $|\Delta|/\nu$, and $\Delta = E_g - \hbar\omega < 0$ in the case of direct optical transitions. One can recast Eq. (8) in a similar form via the extinction coefficient \mathcal{K} [see Appendix B 1],

$$\mathcal{K} = \frac{2 \sum_{\mathbf{k}, \mathbf{k}', \mathbf{q}'} W_{\mathbf{k}, \mathbf{k}'}^{sc}(\mathbf{e}) f_0(E_{c,\mathbf{k}'}) [1 - f_0(E_{c,\mathbf{k}})]}{\mathcal{N}(c/n)}, \quad (16)$$

that describes light attenuation in the system due to the scattering with n being the refractive index of the crystal, and $\mathcal{N} = In/(\hbar\omega c)$ being the number of photons in the electromagnetic wave, namely,

$$j_{\alpha}^{scatt} = e \frac{\mathcal{K} I}{\hbar\omega} D_{\alpha\beta} \hat{n}_{\beta} P_{circ} \frac{2|\Delta| \tau_p}{3\hbar} \frac{\Phi(\nu)}{\tilde{\Phi}(\nu)}, \quad (17)$$

with $\tilde{\Phi}(\nu) = \pi \sqrt{\nu} / [2(1 + \sqrt{\nu})^3]$. Since the factors ν^2 and $\Phi/\tilde{\Phi} \sim 1$ for the same value of detuning the traditional and Raman photocurrents differ by the factor $\sim \mathcal{A}/\mathcal{K}$ which provides an estimate of the ratio of the electronic transition rates at the light absorption and scattering, respectively. Hence, the RPGE is several orders of magnitude smaller compared to the PGE at the light absorption, see Appendix E for detailed estimates both for bulk semiconductors and for quantum well structures. The RPGE can be further increased stimulating light scattering by an additional beam [37,42,43] and coupling with plasmonic structures [44,45].

B. Photocurrent caused by the wave-vector-linear terms in electron dispersion

We also note that in gyrotropic semiconductors and nanostructures k -linear terms are present in the effective Hamiltonian of the charge carriers due to the spin-orbit coupling [5,7,46,47],

$$\mathcal{H}_{SO} = \hbar \beta_{\alpha\mu} k_{\alpha} \sigma_{\mu}, \quad (18)$$

where $\sigma/2$ is the electron spin operator. These terms provide an additive mechanism for the RPGE current generation. It

can be also described by the general Eq. (5) with

$$\bar{v}_\alpha \sim \beta_{\alpha\mu} \hat{n}_\mu P_{\text{circ}}.$$

The k -linear terms are also responsible for the spin-current generation at Raman scattering [48,49].

C. Role of real electronic transitions in DC current generation

Equations (15) and (17) can be brought to the form of general Eq. (5) with

$$\bar{v}_\alpha \sim \frac{\Delta}{\hbar} D_{\alpha\beta} \hat{n}_\beta P_{\text{circ}}. \quad (19)$$

Equations (5), (17), and (19) demonstrate that even for transparent media, real electronic transitions should occur to enable the photocurrent. In this regard, it is instructive to make several comments about photocurrents for $\hbar\omega$ in the transparency region of the crystal related to recent preprints [35,36]. We reiterate that in the absence of any real electronic transitions DC current is forbidden. It is obvious from general reasons: If a DC current is generated then this current results in a Joule heat in the sample or in the external circuit connected to the sample. It is forbidden by the energy conservation law in the absence of real transitions. On the microscopic level, the absence of the DC photocurrent follows from the arguments presented in Ref. [33]: Without of real transitions the only effect of the field is the renormalization of single-particle dispersion $E_{c,k} \rightarrow \tilde{E}_{c,k}$. During the transient processes of energy and momentum relaxation the distribution function relaxes to an equilibrium function $f_0(\tilde{E}_{c,k})$ of the renormalized dispersion. The DC current would be

$$j_{\text{dc}} = 2 \sum_k \tilde{v}_k f_0(\tilde{E}_{c,k}) = 0, \quad (20)$$

where $\tilde{v}_k = \hbar^{-1} \partial \tilde{E}_{c,k} / \partial k$. Thus, real electronic transitions are crucial for the photocurrent generation.

In the case considered in our paper the real transitions are induced by the light scattering (this point was mentioned in Ref. [35]). In a recent preprint [36] the authors discussed the photocurrent in the optical gap of a metal related to the ‘‘Berry curvature dipole’’ and the ‘‘jerk’’ effects. In this regard, two comments are due:

(i) At linear polarization no current can be generated in the absence of absorption or scattering processes. It follows from the general relation (1) which explicitly shows that the tensor χ responsible for the linear PGE is *odd* at the time reversal. Thus, it contains odd numbers of dissipative constants meaning that real electronic transitions indeed occur in this situation.

(ii) The Berry curvature dipole contribution, at first glance, seems dissipationless: It appears at the circular polarization and does not vanish in the clean limit ($\Gamma \rightarrow 0$ in the terminology of the authors of Ref. [36]). However, as demonstrated in Ref. [12], this contribution is related to the interference of *real* electronic transition processes with the intermediate states in the same (conduction) band (Drude-like absorption) and with the intermediate states in the remote (valence) band. We also note that there is a side-jump contribution to the PGE which differs from the Berry curvature dipole contri-

bution by a numerical factor only. Obviously, real transitions require dissipation, and as the authors of Ref. [36] explicitly check, these processes do not violate basic thermodynamic principles. Note that the absence of scattering rates in the expressions for the Berry curvature dipole and side-jump contributions is due to the cancellation of the rates in product of the Drude transition probability and in the momentum scattering time entering the general expression for the photocurrent, Eq. (5) where for Drude-like transitions $\dot{N} \propto 1/\tau_p$ at $\omega\tau_p \gg 1$.

Generally, the RPGE can be superimposed over the PGE caused by the Drude-like intraband absorption in narrow-gap semiconductors and metals. The RPGE current can be separated experimentally owing to its increase with increasing the light frequency, whereas the intraband absorption decreases with increasing the ω .

VI. CONCLUSION

We have shown that the light scattering results in the steady-state current in noncentrosymmetric media providing a link between the basic processes of light scattering and DC current generation. The RPGE current is generated even if the light is propagating in the transparency spectral region of the crystal. Whereas absorption is absent in this case, the current results from real electronic transitions owing to the Raman scattering of photons by free charge carriers demonstrating the importance of real transitions for a DC current generation in nonabsorbing media. These transitions cause asymmetric distribution of electrons and also quantum shifts. We have identified key mechanisms of the Raman-scattering-induced circular photocurrent for the photon energies slightly below the band gap of a semiconductor and studied the photocurrent generation under intersubband scattering in quantum well structures.

ACKNOWLEDGMENTS

We are grateful to Y. Onishi for valuable discussions. We acknowledge support from the Russian Science Foundation: Projects No. 22-12-00211 (general theory of RPGE, M.M.G.) and No. 22-12-00125 (calculations of RPGE currents, L.E.G.). L.E.G. also thanks the Foundation for the Advancement of Theoretical Physics and Mathematics ‘‘BASIS.’’

APPENDIX A: DIAGRAMMATIC APPROACH TO RPGE

It is instructive to consider the circular photocurrent generation in the diagrammatic approach.

Figure 4(a) shows the diagram relevant for the circular photogalvanic effect (CPGE) at the light absorption. Taking into account that in the absorption region of the spectrum $\hbar\omega \geq E_g$ the energy conservation law can be fulfilled, Fig. 4(a) can be immediately calculated and represents the conduction-band contribution to the photocurrent Eq. (B11). In the absence of absorption this diagram vanishes.

Diagrams 4(b)–4(d) describe the RPGE: These diagrams take into account the photon scattering, i.e., the emission of the secondary photon; the wavy line marked as $\hbar\omega'$. The

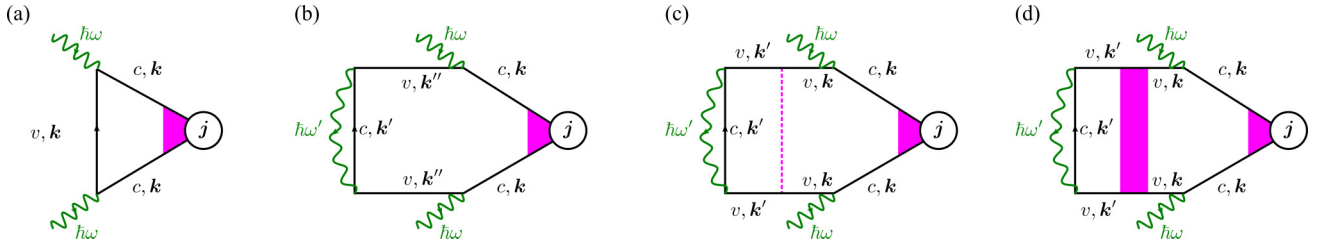


FIG. 4. Diagrams relevant for the photocurrent generation (in-scattering terms).

diagram Fig. 4(b) and its counterpart Fig. 5 describe the RPGE with allowance for the photon momentum. Note that \mathbf{k} , \mathbf{k}' , and \mathbf{k}' are related by the momentum conservation law. Figure 4(c) (and the diagram, analogous to that in Fig. 5) describe the photocurrent with allowance for the scattering in the valence band. The sum of all relevant diagrams with (0, 1, 2, ...) scattering is depicted in Fig. 4(d).

Figure 6 shows the diagrams relevant for the RPGE at the intersubband resonant scattering in quantum well structures. Here extra scattering in the valence band is not required, see Eq. (12).

APPENDIX B: BALLISTIC CIRCULAR PHOTOCURRENT IN BULK GYROTROPIC SEMICONDUCTOR

Substituting the scattering rate (6) with the squared matrix element (7) into Eq. (4a) we obtain the ballistic photocurrent in the form

$$j_\alpha = \frac{e}{V_0} |M_0|^2 |M^{em}|_\Sigma^2 D_{\alpha\beta} i [\mathbf{e} \times \mathbf{e}^*]_\beta \frac{8\pi}{3\hbar^2} I \frac{n_i |V|^2}{V_0} \times \sum_{\mathbf{k}, \mathbf{k}', \mathbf{q}'} \frac{\tau_p(E_{c,\mathbf{k}}) E_{c,\mathbf{k}} f_0(E_{c,\mathbf{k}'}) [1 - f_0(E_{c,\mathbf{k}})]}{(\hbar\omega - E_{c,\mathbf{k}} + E_{v,\mathbf{k}})^2 (\hbar\omega - E_{c,\mathbf{k}} + E_{v,\mathbf{k}'})^2} \times \delta(\hbar\omega - \hbar\omega' - E_{c,\mathbf{k}} + E_{c,\mathbf{k}'}). \quad (\text{B1})$$

Here we assumed the parabolic dispersion $E_{c,\mathbf{k}} = \hbar^2 k^2 / 2m_e$ with m_e being the effective mass. Here $|M^{em}|_\Sigma^2$ is the emission matrix element summed over the secondary photon polarization. In calculation of $|M^{em}|_\Sigma^2$ we can disregard \mathbf{k}' -linear terms because they are sensitive to \mathbf{e}' , we also disregard k'^2 and higher-order contributions to the matrix elements. Note that $M^{abs}(\mathbf{e})$ describes the stimulated process (we consider classical electromagnetic wave incident on the sample), whereas the emission process is spontaneous. That is why we use different

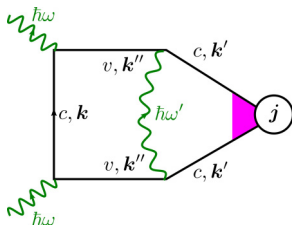


FIG. 5. Second diagram describing the RPGE with allowance for the photon wave vector (out-scattering term).

normalizations of M^{em} and M^{abs} , see the main text below Eq. (6) for details.

For the following calculations we perform the summation over \mathbf{q}' by means of the energy conservation δ function:

$$j_\alpha = \frac{e}{V_0} D_{\alpha\beta} i [\mathbf{e} \times \mathbf{e}^*]_\beta \frac{4}{3\hbar} I \frac{n_i |M_0 V|^2}{V_0} \gamma_r \times \sum_{\mathbf{k}, \mathbf{k}'} \frac{\tau_p(E_{c,\mathbf{k}}) E_{c,\mathbf{k}} f_0(E_{c,\mathbf{k}'}) [1 - f_0(E_{c,\mathbf{k}})]}{(\hbar\omega - E_{c,\mathbf{k}} + E_{v,\mathbf{k}})^2 (\hbar\omega - E_{c,\mathbf{k}} + E_{v,\mathbf{k}'})^2}, \quad (\text{B2})$$

where we introduced the rate of emission of the secondary photon (i.e., the recombination rate of the electron-hole pair in the vicinity of the fundamental band gap),

$$\gamma_r = \frac{2\pi}{\hbar} |M^{em}|_\Sigma^2 \sum_{\mathbf{q}'} \delta(\hbar\omega - \hbar\omega' - E_{c,\mathbf{k}} + E_{c,\mathbf{k}'}).$$

Further calculations can be simplified as follows: We sum over \mathbf{k}' (initial electron wave vector) under the assumption that $E_F, T \ll E_g - \hbar\omega$ (T is the temperature expressed in the energy units). Hence, the \mathbf{k}' dependence of the denominators can be neglected in this case. This summation yields $n_e V_0 / 2$ with $n_e = (2/V_0) \sum_{\mathbf{k}'} f_0(E_{c,\mathbf{k}'})$ being the electron density. Under the same assumption one can omit $1 - f_0(E_{c,\mathbf{k}})$ (but keep the \mathbf{k} dependence in the denominators otherwise the integral diverges at large \mathbf{k}), and we finally have

$$j_\alpha = \frac{e}{V_0} D_{\alpha\beta} i [\mathbf{e} \times \mathbf{e}^*]_\beta \frac{2}{3\hbar} I n_e n_i |M_0 V|^2 \gamma_r \times \sum_{\mathbf{k}} \frac{\tau_p(E_{c,\mathbf{k}}) E_{c,\mathbf{k}}}{(\hbar\omega - E_{c,\mathbf{k}} + E_{v,\mathbf{k}})^2 (\hbar\omega - E_{c,\mathbf{k}} + E_{v,\mathbf{k}'})^2}. \quad (\text{B3})$$

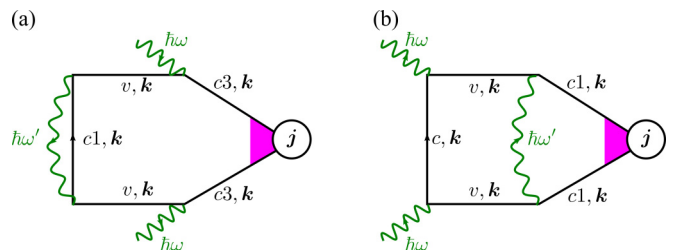


FIG. 6. Diagrams relevant for the RPGE at the intersubband scattering: (a) in-scattering and (b) out-scattering contributions.

Here all energies are counted from the bottom of the conduction band. Using,

$$n_i |V|^2 \tau_p(E_c) = \xi \frac{\hbar}{2\pi g_c(E_c)},$$

$$\sum_k \dots = \mathcal{V}_0 \int_0^\infty dE_c g_c(E_c) \dots,$$

$$E_{c,k} - E_{v,k} = \nu E_{c,k} + E_g, \quad \nu = 1 + \frac{m_e}{m_h}, \quad (\text{B4})$$

$$\int_0^\infty dE_c \frac{E_c}{(\hbar\omega - E_g - \nu E_c)^2 (\hbar\omega - E_g - E_c)^2} = \frac{\Phi(\nu)}{\Delta^2}, \quad \Delta = E_g - \hbar\omega,$$

$$\Phi(\nu) = \int_0^\infty dx \frac{x}{(1 + \nu x)^2 (1 + x)^2} = \frac{(\nu + 1) \ln \nu - 2(\nu - 1)}{(\nu - 1)^3}, \quad \Phi(1) = \frac{1}{6}, \quad (\text{B6})$$

we finally get Eq. (8),

$$j_\alpha = en_e \gamma_r D_{\alpha\beta} i [\mathbf{e} \times \mathbf{e}^*]_\beta I \frac{|M_0|^2 \xi \Phi(\nu)}{\Delta^2} \frac{1}{3\pi}. \quad (\text{B7})$$

1. Light extinction and RPGE

Let us introduce the extinction coefficient \mathcal{K} [cm^{-1}] related to the light scattering,

$$\mathcal{K} = \frac{2 \sum_{\mathbf{k}, \mathbf{k}', \mathbf{q}} W_{\mathbf{k}, \mathbf{k}'}^{sc}(\mathbf{e}) f_0(E_{c, \mathbf{k}'}) [1 - f_0(E_{c, \mathbf{k}})]}{\mathcal{N}(c/n)}. \quad (\text{B8})$$

It describes light attenuation in the system due to the scattering. Here n is the refractive index of the crystal, and \mathcal{N} is the number of photons in the electromagnetic wave. Taking into account that $I = \mathcal{N} \hbar \omega c / n$ and performing a summation over \mathbf{q}' to obtain γ_r , over \mathbf{k}' to obtain n_e , and over \mathbf{k} by virtue of

$$\int_0^\infty dE_c \frac{g_c(E_c)}{(\hbar\omega - E_g - \nu E_c)^2 (\hbar\omega - E_g - E_c)^2} = \tilde{\Phi}(\nu) \frac{g_c(E_\omega)}{E_\omega^3 \nu^3},$$

$$E_\omega = \frac{E_g - \hbar\omega}{\nu}, \quad \tilde{\Phi}(\nu) = \frac{\pi \sqrt{\nu}}{2(1 + \sqrt{\nu})^3},$$

and using $g_c(E_\omega) n_i |V|^2 = \xi \hbar / [2\pi \tau_p(E_\omega)]$, we have

$$\mathcal{K} = n_e \gamma_r \frac{\xi \hbar}{2\pi \tau_p} \tilde{\Phi}(\nu) \frac{\hbar \omega |M_0|^2}{\Delta^3}. \quad (\text{B9})$$

As a result for the Raman-scattering-induced photocurrent we have Eq. (17),

$$j_\alpha^{\text{scatt}} = e \frac{\mathcal{K} I}{\hbar \omega} D_{\alpha\beta} i [\mathbf{e} \times \mathbf{e}^*]_\beta \frac{2 \Delta \tau_p(E_\omega)}{3\hbar} \frac{\Phi(\nu)}{\tilde{\Phi}(\nu)}. \quad (\text{B10})$$

2. Relation to the photogalvanic effect at light absorption

Let us calculate the (ballistic) CPGE current in the same system generated at $\hbar\omega > E_g$. We calculate the electron contribution only (this is the net electric current if the relaxation time in the valence band is very short). The CPGE current

where ξ is the ratio of the conduction- and valence-band elastic-scattering matrix elements squared: $\xi = |V_v|^2 / |V_c|^2$, $g_c(E_c)$ is the density of states in the conduction band, we get

$$j_\alpha = e D_{\alpha\beta} i [\mathbf{e} \times \mathbf{e}^*]_\beta I n_e |M_0|^2 \gamma_r \frac{\xi}{3\pi}$$

$$\times \int_0^\infty dE_c \frac{E_c}{(\hbar\omega - E_g - \nu E_c)^2 (\hbar\omega - E_g - E_c)^2}. \quad (\text{B5})$$

Calculating the integral,

density at light absorption is given by

$$j_\alpha^{\text{abs}} = 2e \sum_k W_k^{\text{abs}}(\mathbf{e}) \tau_p(E_{c, \mathbf{k}}) v_\alpha(\mathbf{k}) \delta(E_{c, \mathbf{k}} - E_{v, \mathbf{k}} - \hbar\omega), \quad (\text{B11})$$

where the asymmetric contribution to the light absorption probability at direct optical transition is

$$W_k^{\text{abs}}(\mathbf{e}) = \frac{2\pi}{\hbar} I |M_0|^2 D_{\alpha\beta} i [\mathbf{e} \times \mathbf{e}^*]_\beta k_\alpha. \quad (\text{B12})$$

Then we obtain

$$j_\alpha^{\text{abs}} = 2e \frac{2\pi}{\hbar} I |M_0|^2 D_{\alpha\beta} i [\mathbf{e} \times \mathbf{e}^*]_\beta$$

$$\times \sum_k \frac{2}{3\hbar} E_{c, \mathbf{k}} \tau_p(E_{c, \mathbf{k}}) \delta(\nu E_{c, \mathbf{k}} + E_g - \hbar\omega)$$

$$= e I D_{\alpha\beta} i [\mathbf{e} \times \mathbf{e}^*]_\beta \frac{8\pi |M_0|^2}{3\hbar^2} g_c(|E_\omega|) \frac{|E_\omega| \tau_p(|E_\omega|)}{\nu^2}$$

$$\times \Theta(\hbar\omega - E_g). \quad (\text{B13})$$

It is convenient to introduce the light absorption coefficient $\mathcal{A}(\omega)$ with the dimension of cm^{-1} related to the direct optical transitions as

$$\mathcal{A} = \frac{\hbar\omega}{I} W_{cv}, \quad (\text{B14})$$

where the direct interband transition rate,

$$W_{cv} = 2 \frac{2\pi}{\hbar} \sum_k I |M_0|^2 \delta(E_{c, \mathbf{k}} - E_{v, \mathbf{k}} - \hbar\omega)$$

$$= \frac{4\pi}{\hbar} I |M_0|^2 \frac{g_c(|E_\omega|)}{\nu} \Theta(\hbar\omega - E_g), \quad (\text{B15})$$

and

$$\mathcal{A} = 4\pi \omega |M_0|^2 \frac{g_c(|E_\omega|)}{\nu} \Theta(\hbar\omega - E_g). \quad (\text{B16})$$

Finally, we obtain from Eq. (B13) the circular photocurrent caused by the CPGE in the form of Eq. (14) of the main text,

$$j_\alpha^{\text{abs}} = e \frac{\mathcal{A} I}{\hbar \omega} D_{\alpha\beta} i [\mathbf{e} \times \mathbf{e}^*]_\beta \frac{2 |E_\omega| \tau_p(|E_\omega|)}{3\nu \hbar}. \quad (\text{B17})$$

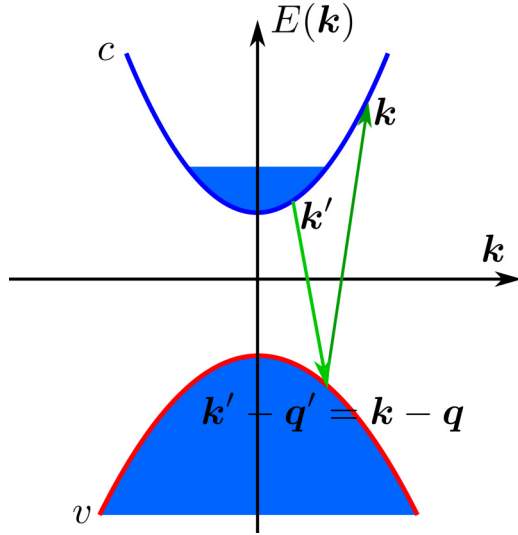


FIG. 7. Scheme of the light scattering process with allowance for the radiation wave vector.

APPENDIX C: ALLOWANCE FOR THE RADIATION WAVE VECTOR IN RPGE

In the previous Appendix we studied the RPGE photocurrent that is generated in a course of a three-step process of virtual photon absorption, valence-band hole scattering, and virtual photon emission. In this way the electron wave vectors in the initial k' and final k states are decoupled. Let us now discuss the contribution to RPGE where the valence-band hole scattering is absent. Such a process takes place with allowance for the photon wave vector, see Fig. 7, this process is the main process of light scattering by free carriers in semiconductors for $\hbar\omega \lesssim E_g$ [5]. Corresponding transition probability is given by

$$W_{k,k'}^q(\mathbf{e}', \mathbf{e}) = \frac{2\pi}{\hbar} \delta(\hbar\omega - \hbar\omega' - E_{c,k} + E_{c,k'}) \delta_{k+q', k'+q} I \times \left| \frac{M_{k'}^{em}(\mathbf{e}') M_k^{abs}(\mathbf{e})}{\hbar\omega - E_{c,k} + E_{v,k}} \right|^2. \quad (\text{C1})$$

Here the Kronecker δ accounts for the momentum conservation in the course of light scattering [Eq. (9) of the main text],

$$\mathbf{k}' + \mathbf{q} = \mathbf{k} + \mathbf{q}'.$$

The photocurrent is given by [cf. Eq. (4a)]

$$\mathbf{j}_b = \frac{2e}{V_0} \sum_{k,k',q'} [\mathbf{v}_k \tau_p(E_{c,k}) - \mathbf{v}_{k'} \tau_p(E_{c,k'})] W_{k,k'}^q(\mathbf{e}) f_0(E_{c,k'}) [1 - f_0(E_{c,k})], \quad (\text{C2})$$

Let us assume for simplicity that the energy dependence of the electron momentum scattering time can be disregarded. In this case the velocity-dependent term in square brackets can be recast as

$$[\mathbf{v}_k \tau_p(E_{c,k}) - \mathbf{v}_{k'} \tau_p(E_{c,k'})] = \tau_p \frac{\hbar}{m_e} (\mathbf{q}' - \mathbf{q}).$$

Note that the difference of velocities in the initial and final states is now small and related to the photon wave vector. It results in suppression of the photocurrent.

Disregarding in Eq. (C2) the \mathbf{q}, \mathbf{q}' dependence of all remaining terms we obtain the polarization-independent photocurrent related to the photon *drag* effect at the Raman scattering,

$$\mathbf{j}_b = \frac{2e}{V_0} \frac{\hbar}{m_e} (-\mathbf{q}) \sum_{k,q'} W_{k,k}^q(\mathbf{e}) f_0(E_{c,k}) [1 - f_0(E_{c,k})]. \quad (\text{C3})$$

According to the time-reversal symmetry this effect is independent of the circular polarization of light.

Furthermore, to obtain the polarization-dependent current we need to extract \mathbf{k} - and \mathbf{q} -linear contributions from the occupancy factors, otherwise, the sum over \mathbf{k} in Eq. (C2) vanishes. The resulting current contains the factor $\sim \hbar^2 q^2 / m_e$ instead of $\sim \xi \hbar / \tau_p$ that appears in Eq. (B3) due to the scattering in the valence band. As a result, the RPGE without scattering in the valence band is smaller than the current in Eq. (B10) by a factor of

$$\sim \frac{\hbar q^2 \tau_p}{m_e}.$$

For typical conditions this factor is small.

APPENDIX D: INTERSUBBAND-SCATTERING-ASSISTED PHOTOCURRENT

In noncentrosymmetric quantum well systems, the intersubband scattering probability of light $W_{3 \leftarrow 1}^{sc}(\mathbf{e}, \mathbf{k})$ contains, in general, an asymmetric part. As a result, there is a ballistic contribution to the photocurrent,

$$\mathbf{j} = \frac{2e}{S_0} \sum_{k,k',q'} [\mathbf{v}_{c3,k} \tau_p(E_{c3,k}) - \mathbf{v}_{c1,k} \tau_p(E_{c1,k})] W_{3 \leftarrow 1}^{sc}(\mathbf{e}, \mathbf{k}) f_0(E_{c1,k}) [1 - f_0(E_{c3,k})], \quad (\text{D1})$$

where S_0 is the normalization area. Substitution of the scattering rate given by Eq. (11) of the main text yields

$$\mathbf{j}_\alpha = \frac{e}{S_0} D_{\alpha\beta} i [\mathbf{e} \times \mathbf{e}^*]_\beta \frac{4\pi}{\hbar^2} I |M_0|^4 \times \sum_{k,q'} \frac{\hbar^2 k^2}{2} \frac{\tau_p(E_{c3,k})/m_{c3} - \tau_p(E_{c1,k})/m_{c1}}{(\hbar\omega - E_{c3,k} + E_{v,k})^2} f_0(E_{c1,k}) \times [1 - f_0(E_{c3,k})] \delta(\hbar\omega - \hbar\omega' - E_{c3,k} + E_{c1,k}). \quad (\text{D2})$$

For the following calculations we perform the summation over \mathbf{q}' by means of the energy conservation δ function:

$$\mathbf{j}_\alpha = \frac{e}{S_0} D_{\alpha\beta} i [\mathbf{e} \times \mathbf{e}^*]_\beta \frac{2}{\hbar} I |M_0|^2 \gamma_r^{\text{QW}} \times \sum_k \frac{\hbar^2 k^2}{2} \frac{\tau_p(E_{c3,k})/m_{c3} - \tau_p(E_{c1,k})/m_{c1}}{(\hbar\omega - E_{c3,k} + E_{v,k})^2} f_0(E_{c1,k}) \times [1 - f_0(E_{c3,k})], \quad (\text{D3})$$

where we introduced the rate of emission of the secondary photon (i.e., the recombination rate of the electron-hole pair

in the vicinity of the fundamental band gap),

$$\gamma_r^{\text{QW}} = \frac{2\pi}{\hbar} |M_0|^2 \sum_{q'} \delta(\hbar\omega - \hbar\omega' - E_{c3,k} + E_{c1,k}).$$

Further calculations can be simplified as follows: we assume $\tau_p(E_{c3,k}) \ll \tau_p(E_{c1,k})$, $f_0(E_{c3,k}) \ll 1$. Then we have

$$j_\alpha = -\frac{e}{S_0} D_{\alpha\beta} i [\mathbf{e} \times \mathbf{e}^*]_\beta \frac{2}{\hbar} I |M_0|^2 \gamma_r^{\text{QW}} \times \sum_k \frac{E_{c1,k} \tau_p(E_{c1,k})}{(\hbar\omega - E_{c3,k} + E_{v,k})^2} f_0(E_{c1,k}). \quad (\text{D4})$$

For crude estimation we can assume $E_F, T \ll E_{g3} - \hbar\omega$, where $E_{g3} = E_g + \Delta_{31}$, and obtain

$$j_\alpha \approx -en_e \gamma_r^{\text{QW}} D_{\alpha\beta} i [\mathbf{e} \times \mathbf{e}^*]_\beta \frac{2(E) \tau_{\text{tr}}}{\hbar} I \frac{|M_0|^2}{(E_{g3} - \hbar\omega)^2}. \quad (\text{D5})$$

More precisely, using

$$\sum_k \dots = S_0 g_{c1} \int_0^\infty dE_{c1} \dots,$$

$$E_{c3,k} - E_{v,k} = \nu_{31} E_{c1,k} + E_{g3}, \quad \nu_{31} = m_{c1} \left(\frac{1}{m_{c3}} + \frac{1}{m_h} \right), \quad (\text{D6})$$

where g_{c1} is the density of states in the first conduction subband, we get

$$j_\alpha = -e D_{\alpha\beta} i [\mathbf{e} \times \mathbf{e}^*]_\beta \frac{2}{\hbar} I |M_0|^2 \gamma_r^{\text{QW}} \frac{\hbar}{2\pi n_i |V|^2} \times \int_0^\infty dE \frac{E}{(\hbar\omega - E_{g3} - \nu_{31}E)^2} f_0(E). \quad (\text{D7})$$

At low temperatures we have

$$\int_0^{E_F} dE \frac{E}{(\hbar\omega - E_{g3} - \nu_{31}E)^2} = \frac{1}{\nu_{31}^2} \left(\ln \frac{1+\varepsilon}{\varepsilon} - \frac{1}{1+\varepsilon} \right), \quad \varepsilon = \frac{E_{g3} - \hbar\omega}{\nu_{31} E_F}, \quad (\text{D8})$$

whereas the electron concentration is given by $n_e = 2g_{c1} E_F$. Therefore, we get for Fermi statistics [when $\tau_{\text{tr}} = \tau_p(E_F)$] Eqs. (13) and (14),

$$j_\alpha = -en_e \gamma_r^{\text{QW}} D_{\alpha\beta} i [\mathbf{e} \times \mathbf{e}^*]_\beta I \frac{|M_0|^2 \tau_{\text{tr}}}{\nu_{31}^2 \hbar E_F} \left(\ln \frac{1+\varepsilon}{\varepsilon} - \frac{1}{1+\varepsilon} \right). \quad (\text{D9})$$

At Boltzmann statistics we have

$$\begin{aligned} & \int_0^\infty dE \frac{E f_0(E)}{(\hbar\omega - E_{g3} - \nu_{31}E)^2} \\ &= \frac{\exp(\mu/T)}{\nu_{31}^2} \int_0^\infty dx \frac{x \exp(-x)}{(x+b)^2} \\ &= \frac{\exp(\mu/T)}{\nu_{31}^2} [e^b \text{Ei}(-b)(1+b) - 1], \end{aligned} \quad (\text{D10})$$

where $\text{Ei}(x) = \int_{-x}^\infty t^{-1} \exp(-t) dt$ is the exponential integral,

$$b = \frac{E_{g3} - \hbar\omega}{\nu_{31} T}, \quad n_e = 2g_{c1} T \exp(\mu/T). \quad (\text{D11})$$

As a result, we obtain

$$j_\alpha = -en_e \gamma_r^{\text{QW}} D_{\alpha\beta} i [\mathbf{e} \times \mathbf{e}^*]_\beta I \frac{|M_0|^2 \tau_p(T)}{\nu_{31}^2 \hbar T} \times [e^b \text{Ei}(-b)(1+b) - 1]. \quad (\text{D12})$$

APPENDIX E: COMPARISON OF RPGE WITH PHOTOCURRENT IN THE ABSORPTION REGION

First, we present estimations of the RPGE and its comparison with the CPGE in the absorption region in the case of bulk system. Taking $\xi = 1$, $\nu = 1$, and, hence, $E_\omega \equiv \Delta/\nu = \Delta$, and omitting the factor $\Phi(\nu) \sim 1$ we obtain from Eqs. (8) and (B13) the estimate,

$$\frac{j^{\text{scatt}}}{j^{\text{abs}}} \sim \frac{1}{12\pi^2} \left(\frac{E_F}{\Delta} \right)^{3/2} \frac{\gamma_r}{(\Delta/\hbar)^2 \tau_p}. \quad (\text{E1})$$

We recall that the relation $E_F \ll \Delta$ was assumed in derivation of RPGE, see the main text for details. Taking $E_F/\Delta = 1/3$ we get

$$\begin{aligned} \frac{j^{\text{scatt}}}{j^{\text{abs}}} &\sim 1.6 \times 10^{-3} \frac{\gamma_r}{(\Delta/\hbar)^2 \tau_p} \\ &= 0.7 \times 10^{-9} \frac{\gamma_r \times 10 \text{ ns}}{(\Delta/10 \text{ meV})^2 \tau_p/\text{ps}}. \end{aligned} \quad (\text{E2})$$

Note that at $\Delta = 10 \text{ meV}$ and $\tau_p = 1 \text{ ps}$ the parameter $\Delta \tau_p/\hbar = 15.2$, so $E_F \tau_p/\hbar \approx 5$.

Let us now turn to the case of a quantum well structure. At the intersubband scattering, we obtain from Eqs. (D5) and (B13) [with the coefficient $8/3 \rightarrow 4$ taking into account appropriate averaging in the two-dimensional case] with $\nu = 1$,

$$\frac{j^{\text{scatt}}}{j^{\text{abs}}} \approx \frac{1}{2\pi} \left(\frac{E_F}{\Delta_{\text{QW}}} \right)^2 \frac{\hbar \gamma_r^{\text{QW}}}{\Delta}. \quad (\text{E3})$$

Here we used $n_e = 2g_c E_F$. We recall that $\Delta = \hbar\omega - E_g$ and $\Delta_{\text{QW}} = E_{g3} - \hbar\omega$. At $E_F/\Delta_{\text{QW}} = 1/3$, $\Delta = 10 \text{ meV}$, and $1/\gamma_r = 10 \text{ ns}$ we get the estimate for the photocurrent ratio 1.2×10^{-7} .

[1] A. M. Glass, D. von der Linde, and T. J. Negran, High-voltage bulk photovoltaic effect and the photorefractive process in LiNbO_3 , *Appl. Phys. Lett.* **25**, 233 (1974).

[2] E. L. Ivchenko and G. E. Pikus, New photogalvanic effect in gyrotropic crystals, *JETP Lett.* **27**, 640 (1978).

[3] V. I. Belinicher, Space-oscillating photocurrent in crystals without symmetry center, *Phys. Lett. A* **66**, 213 (1978).

- [4] B. I. Sturman and V. M. Fridkin, *The Photovoltaic and Photo-refractive Effects in Non-centrosymmetric Materials* (Gordon and Breach, New York, 1992).
- [5] E. L. Ivchenko, *Optical Spectroscopy of Semiconductor Nanostructures* (Alpha Science, Harrow, UK, 2005).
- [6] S. D. Ganichev and W. Prettl, Spin photocurrents in quantum wells, *J. Phys.: Condens. Matter* **15**, R935 (2003).
- [7] *Spin Physics in Semiconductors*, 2nd ed., edited by M. I. Dyakonov, Springer Series in Solid-State Sciences Vol. 157 (Springer, Berlin, 2017).
- [8] M. M. Glazov and S. D. Ganichev, High frequency electric field induced nonlinear effects in graphene, *Phys. Rep.* **535**, 101 (2014).
- [9] J. E. Moore and J. Orenstein, Confinement-Induced Berry Phase and Helicity-Dependent Photocurrents, *Phys. Rev. Lett.* **105**, 026805 (2010).
- [10] T. Morimoto and N. Nagaosa, Topological aspects of nonlinear excitonic processes in noncentrosymmetric crystals, *Phys. Rev. B* **94**, 035117 (2016).
- [11] F. de Juan, A. G. Grushin, T. Morimoto, and J. E. Moore, Quantized circular photogalvanic effect in Weyl semimetals, *Nat. Commun.* **8**, 15995 (2017).
- [12] L. E. Golub, E. L. Ivchenko, and B. Spivak, Semiclassical theory of the circular photogalvanic effect in gyrotropic systems, *Phys. Rev. B* **102**, 085202 (2020).
- [13] J. Orenstein, J. Moore, T. Morimoto, D. Torchinsky, J. Harter, and D. Hsieh, Topology and symmetry of quantum materials via nonlinear optical responses, *Annu. Rev. Condens. Matter Phys.* **12**, 247 (2021).
- [14] S. D. Ganichev, W. Weber, J. Kiermaier, S. N. Danilov, P. Olbrich, D. Schuh, W. Wegscheider, D. Bougeard, G. Abstreiter, and W. Prettl, All-electric detection of the polarization state of terahertz laser radiation, *J. Appl. Phys.* **103**, 114504 (2008).
- [15] S. N. Danilov, B. Wittmann, P. Olbrich, W. Eder, W. Prettl, L. E. Golub, E. V. Beregulin, Z. D. Kvon, N. N. Mikhailov, S. A. Dvoretzky, V. A. Shalygin, N. Q. Vinh, A. F. G. van der Meer, B. Murdin, and S. D. Ganichev, Fast detector of the ellipticity of infrared and terahertz radiation based on HgTe quantum well structures, *J. Appl. Phys.* **105**, 013106 (2009).
- [16] V. M. Asnin, A. A. Bakun, A. M. Danishevskii, E. L. Ivchenko, G. E. Pikus, and A. A. Rogachev, Observation of a photo-emf that depends on the sign of the circular polarization of light, *JETP Lett.* **28**, 80 (1978).
- [17] S. D. Ganichev, E. L. Ivchenko, S. N. Danilov, J. Eroms, W. Wegscheider, D. Weiss, and W. Prettl, Conversion of Spin into Directed Electric Current in Quantum Wells, *Phys. Rev. Lett.* **86**, 4358 (2001).
- [18] S. Ganichev, E. Ivchenko, and W. Prettl, Photogalvanic effects in quantum wells, *Physica E* **14**, 166 (2002).
- [19] B. Wittmann, S. N. Danilov, V. V. Bel'kov, S. A. Tarasenko, E. G. Novik, H. Buhmann, C. Brüne, L. W. Molenkamp, Z. D. Kvon, N. N. Mikhailov, S. A. Dvoretzky, N. Q. Vinh, A. F. G. van der Meer, B. Murdin, and S. D. Ganichev, Circular photogalvanic effect in HgTe/CdHgTe quantum well structures, *Semicond. Sci. Technol.* **25**, 095005 (2010).
- [20] J. W. McIver, D. Hsieh, H. Steinberg, P. Jarillo-Herrero, and N. Gedik, Control over topological insulator photocurrents with light polarization, *Nat. Nanotechnol.* **7**, 96 (2012).
- [21] P. Olbrich, L. E. Golub, T. Herrmann, S. N. Danilov, H. Plank, V. V. Bel'kov, G. Mussler, C. Weyrich, C. M. Schneider, J. Kampmeier, D. Grützmacher, L. Plucinski, M. Eschbach, and S. D. Ganichev, Room-temperature high-frequency transport of Dirac fermions in epitaxially grown Sb₂Te₃- and Bi₂Te₃-based topological insulators, *Phys. Rev. Lett.* **113**, 096601 (2014).
- [22] H. Plank, L. E. Golub, S. Bauer, V. V. Bel'kov, T. Herrmann, P. Olbrich, M. Eschbach, L. Plucinski, C. M. Schneider, J. Kampmeier, M. Lanius, G. Mussler, D. Grützmacher, and S. D. Ganichev, Photon drag effect in (Bi_{1-x}Sb_x)₂Te₃ three-dimensional topological insulators, *Phys. Rev. B* **93**, 125434 (2016).
- [23] M. V. Durnev and S. A. Tarasenko, High-frequency nonlinear transport and photogalvanic effects in 2D topological insulators, *Ann. Phys.* **531**, 1800418 (2019).
- [24] N. V. Leppenpen and L. E. Golub, Nonlinear optical absorption and photocurrents in topological insulators, *Phys. Rev. B* **105**, 115306 (2022).
- [25] Q. Ma, S.-Y. Xu, C.-K. Chan, C.-L. Zhang, G. Chang, Y. Lin, W. Xie, T. Palacios, H. Lin, S. Jia, P. A. Lee, P. Jarillo-Herrero, and N. Gedik, Direct optical detection of Weyl fermion chirality in a topological semimetal, *Nat. Phys.* **13**, 842 (2017).
- [26] D. Rees, K. Manna, B. Lu, T. Morimoto, H. Borrmann, C. Felser, J. E. Moore, D. H. Torchinsky, and J. Orenstein, Helicity-dependent photocurrents in the chiral Weyl semimetal RhSi, *Sci. Adv.* **6**, eaba0509 (2020).
- [27] C. Drexler, S. A. Tarasenko, P. Olbrich, J. Karch, M. Hirmer, F. Müller, M. Gmitra, J. Fabian, R. Yakimova, S. Lara-Avila, S. Kubatkin, M. Wang, R. Vajtai, P. Ajayan, J. Kono, and S. D. Ganichev, Magnetic quantum ratchet effect in graphene, *Nat. Nanotechnol.* **8**, 104 (2013).
- [28] S. Candussio, M. V. Durnev, S. Slizovskiy, T. Jötten, J. Keil, V. V. Bel'kov, J. Yin, Y. Yang, S.-K. Son, A. Mishchenko, V. Fal'ko, and S. D. Ganichev, Edge photocurrent in bilayer graphene due to inter-Landau-level transitions, *Phys. Rev. B* **103**, 125408 (2021).
- [29] S. Candussio, L. E. Golub, S. Bernreuter, T. Jötten, T. Rockinger, K. Watanabe, T. Taniguchi, J. Eroms, D. Weiss, and S. D. Ganichev, Nonlinear intensity dependence of edge photocurrents in graphene induced by terahertz radiation, *Phys. Rev. B* **104**, 155404 (2021).
- [30] J. Quereda, T. S. Ghiasi, J.-S. You, J. van den Brink, B. J. van Wees, and C. H. van der Wal, Symmetry regimes for circular photocurrents in monolayer MoSe₂, *Nat. Commun.* **9**, 3346 (2018).
- [31] A. Rasmita, C. Jiang, H. Ma, Z. Ji, R. Agarwal, and W. bo Gao, Tunable geometric photocurrent in van der waals heterostructure, *Optica* **7**, 1204 (2020).
- [32] R. Asgari and D. Culcer, Unidirectional valley-contrasting photocurrent in strained transition metal dichalcogenide monolayers, *Phys. Rev. B* **105**, 195418 (2022).
- [33] V. I. Belinicher, E. L. Ivchenko, and G. E. Pikus, Transient photocurrent in gyrotropic crystals, *Sov. Phys. - Semicond.* **20**, 558 (1986).
- [34] L. E. Golub and E. L. Ivchenko, Circular and magnetoinduced photocurrents in Weyl semimetals, *Phys. Rev. B* **98**, 075305 (2018).

- [35] Y. Onishi, H. Watanabe, T. Morimoto, and N. Nagaosa, Photovoltaic effect in noncentrosymmetric material without optical absorption, [arXiv:2204.12727](#).
- [36] L. Shi, O. Matsyshyn, J. C. W. Song, and I. S. Villadiejo, The Berry dipole photovoltaic demon and the thermodynamics of photo-current generation within the optical gap of metals, [arXiv:2207.03496](#).
- [37] *Light Scattering in Solids*, edited by M. Cardona (Springer-Verlag, Berlin/Heidelberg, 1975).
- [38] C. Schüller, *Inelastic Light Scattering of Semiconductor Nanostructures* (Springer, Berlin/Heidelberg, 2006).
- [39] V. I. Belinicher, E. L. Ivchenko, and B. I. Sturman, Kinetic theory of the displacement photovoltaic effect in piezoelectrics, *JETP* **56**, 359 (1982).
- [40] B. I. Sturman, Ballistic and shift currents in the bulk photovoltaic effect theory, *Phys.-Usp.* **63**, 407 (2020).
- [41] L. E. Golub and E. L. Ivchenko, Shift photocurrent induced by two-quantum transitions, *J. Exp. Theor. Phys.* **112**, 152 (2011).
- [42] G. Eckhardt, R. W. Hellwarth, F. J. McClung, S. E. Schwarz, D. Weiner, and E. J. Woodbury, Stimulated Raman Scattering From Organic Liquids, *Phys. Rev. Lett.* **9**, 455 (1962).
- [43] R. C. Prince, R. R. Frontiera, and E. O. Potma, Stimulated raman scattering: From bulk to nano, *Chem. Rev.* **117**, 5070 (2017).
- [44] M. Fleischmann, P. Hendra, and A. McQuillan, Raman spectra of pyridine adsorbed at a silver electrode, *Chem. Phys. Lett.* **26**, 163 (1974).
- [45] B. Sharma, R. R. Frontiera, A.-I. Henry, E. Ringe, and R. P. Van Duyne, Sers: Materials, applications, and the future, *Mater. Today* **15**, 16 (2012).
- [46] E. I. Rashba and V. I. Sheka, Symmetry of energy bands in crystals of wurtzite type. II. Symmetry of bands with spin-orbit interaction included, *Fiz. Tverd. Tela: Collected Papers* **2**, 162 (1959).
- [47] S. D. Ganichev and L. E. Golub, Interplay of Rashba/Dresselhaus spin splittings probed by photogalvanic spectroscopy—A review, *Phys. Status Solidi B* **251**, 1801 (2014).
- [48] A. Najmaie, E. Y. Sherman, and J. E. Sipe, Generation of Spin Currents via Raman Scattering, *Phys. Rev. Lett.* **95**, 056601 (2005).
- [49] A. Najmaie, E. Y. Sherman, and J. E. Sipe, Raman mechanism for spin-current generation in a two-dimensional electron gas, *Phys. Rev. B* **72**, 041304(R) (2005).